Implementation of Start-up/Shutdown Model into Alkali Metal Heat Pipe Analysis Code

Ye Sung Kim, San Lee, Hyoung Kyu Cho*
Department of nuclear engineering, Seoul National Univ., 1 Gwanak-ro, Gwanak-gu, Seoul 08826
**Corresponding author: chohk@snu.ac.kr*

***Keywords :** alkali metal heat pipe, high temperature heat pipe, heat pipe start-up, heat pipe cooled microreactor.

1. Introduction

In recent years, as needs for active measures against climate change and decentralized power grids for remote areas and industrial complexes emerged, researches on SMR and microreactor have increased [1] [2]. Among these, heat pipe cooled microreactor (HPMR) stands out, employing heat pipes to passively remove heat generated in the solid reactor core. The absence of pumps and valves for reactor cooling in HPMRs makes them advantageous for miniaturization and ensures high system stability [3].

Many HPMR designs apply alkali metal heat pipes to remove large heat under high temperature condition, which is normal operation condition for working fluids such as Na, K [4] [5]. However, these working fluids are frozen under room-temperature condition, making the heat pipe inactive while it is not fully heated. Thus, the start-up and shutdown behavior of alkali metal heat pipe should be considered properly to analyze safety issues of HPMR during start-up and shutdown process.

In previous study, to perform more accurate transient analysis including conduction through heat pipe walls, SNU in-house code was developed which is capable of 2-dimensional transient calculation on cylindrical heat pipe [6]. Using this code, the transient heat pipe calculation with axial conduction was performed.

In this study, start-up/shutdown model for alkali metal heat pipe was developed and added to the in-house code. The start-up/shutdown model includes solid-liquid phase change model for the working fluid and heat transfer through wick-vapor interface. The improved heat pipe analysis code was verified with an analytic solution from a lumped heat pipe model and validated with a heat pipe transient operation experiment data.

2. Numerical model for start-up analysis

The heat pipe analysis code used in this study is based on the thermal resistance network model. Assuming azimuthal symmetry, 2-dimensional mesh structure is set to calculate radial and axial heat transfer. Vapor core uses only one cell and is in contact with the innermost layer of the wick.

Working fluid of alkali metal heat pipe stays frozen under room-temperature condition. During start-up and shutdown process, melting and solidification of the working fluid in wick region and development of vapor flow largely affect the transient behavior of the heat pipe. To consider these in the code, solid-liquid phase change model and wick-vapor interface thermal resistances were implemented into the code.

2.1. solid-liquid phase change model

Solid-liquid phase change model using effective heat capacity method was applied to the wick cells to consider latent heat of fusion of the working fluid. Using effective heat capacity method, the given temperature range around melting point was set as mushy zone. Working fluid inside the mushy zone temperature range ($T_m - \delta T \le T \le T_m + \delta T$) was considered as a mixture of solid and liquid state. In this research, linearity between temperature and mass fraction of liquid within the mushy zone was assumed. Therefore, the liquid mass fraction in one cell could be expressed in terms of temperature, as shown in Eq. (1),

$$x = \frac{T - T_m + \delta T}{2\delta T} \quad (T_m - \delta T \le T \le T_m + \delta T) \quad (1)$$

where x is the liquid fraction of a cell, T_m is melting point, and δT is half of the mushy zone temperature range.

By implementing solid-liquid phase change model to the code, the phase of working fluid at a wick cell could be known from the temperature. Specific heat including latent heat effect is given in Eq. (2),

$$C = \begin{cases} C_s & (T < T_m - \delta T) \\ \dfrac{H_{fus}}{2\delta T} + \dfrac{C_s + C_l}{2} & (T_m - \delta T \le T \le T_m + \delta T) \\ C_l & (T > T_m + \delta T) \end{cases} \quad (2)$$

where C_s, C_l are specific heat of solid and liquid phase and H_{fus} is the latent heat of fusion.

However, the calculation may disregard the latent heat of fusion if the temperature difference between the cells is larger than the mushy zone temperature range. To prevent skipping the mushy zone during calculation, Hsiao's method was applied in the solid-liquid phase change model [7]. In a simple 2-dimensional mesh structure, 4 adjacent cells' data were used to evaluate the amount of additional specific heat in one cell, as shown in Eqs. (3). (4),

$$C(T_{i,j}) = \frac{1}{4}\left[C(T_{i,j}, T_{i,j-1}) + C(T_{i,j}, T_{i-1,j}) + C(T_{i,j}, T_{i+1,j}) + C(T_{i,j}, T_{i,j+1})\right] \quad (3)$$

$$C(T_1, T_2) = \frac{1}{T_2 - T_1}\int_{T_1}^{T_2} C(T)dT \quad (4)$$

where $T_{i,j}$ is temperature of i-th cell in axial direction, and j-th cell in radial direction.

2.2. Wick-vapor interface thermal resistance

At the interface between vapor core and wick, phase change (evaporation and condensation) and radiation are the dominant heat transfer mechanisms. And since the vapor core was assumed to be saturated during a single time step, the Clausius – Clapeyron equation on a saturated vapor was used accordingly to calculate heat transfer rate by the phase change [8]. The interfacial thermal resistance due to phase change R_{pc} is given in Eq. (5), where R, P_{sat}, h_{fg} are gas constant, saturation pressure, and latent heat of vaporization of sodium vapor, and A is area of the wick – vapor interface.

$$R_{pc} = \frac{\sqrt{2\pi}R^{1.5}T_v^{2.5}}{P_{sat}h_{fg}^2 A} \quad (5)$$

The amount of heat released by radiation could be obtained through the emissivity and temperature of the wick and vapor core. The amount of heat actually transferred from the wick to the vapor core and vice versa was corrected using the Knudsen number. The thermal resistance due to radiation at the wick-vapor interface R_{rad} can be obtained from Eq. (6), where Kn is Knudsen number, σ is Stefan-Boltzmann constant, ϵ is emissivity of sodium, T_{wi} and T_v are temperature of wick and vapor cell, and A is area of the wick – vapor interface.

$$R_{rad} = \frac{Kn}{\sigma\epsilon(T_{wi} + T_v)(T_{wi}^2 + T_v^2)A} \quad (6)$$

$$Kn = \frac{\mu_v}{\rho_v L^*}\sqrt{\frac{\pi M}{k_B T_v}} \quad (7)$$

The Knudsen number is defined as a ratio between the mean free path and the characteristic length of the system. For the heat pipe vapor core, diameter of the vapor core is the characteristic length L^* [9]. Knudsen number is obtained with Eq. (7), where μ_v, ρ_v, M, T_v are dynamic viscosity, density, atomic mass, and temperature of sodium vapor, and k_B is Boltzmann constant.

2.3. Operation limit

A heat pipe can reach operation limits during start-up when the heat pipe is not fully activated. 5 operation limits were considered in this study, which are viscous, sonic, entrain, capillary and boiling limit. Operation limits can be calculated from heat pipe geometry, material properties of wall, wick, and working fluid, and the vapor temperature [10] [11].

When the heat pipe reached operation limits during the calculation, the interfacial thermal resistance due to the phase change of working fluid was adjusted and the heat transfer rate was re-calculated. By using the ratio between the pervious heat transfer rate and the lowest operation limit as a coefficient for thermal resistance, the excessive heat transfer was cut off by the operation limits.

Since radiative heat transfer at the wick–vapor interface is not affected by operation limit, the thermal resistance due to phase change was adjusted merely by the operation limits.

3. Results and discussion

3.1. Verification of solid-liquid phase change model

1-dimensional Stefan problem was solved to verify the solid-liquid phase change model. Calculation conditions of the problem are listed in Table 1. To set an appropriate mushy zone temperature range, 4 different mushy zone temperature ranges (0.2 K, 1.0 K, 2.0 K, 3.0 K) were used and compared with an analytic solution [12].

Table 1. Calculation conditions for Stefan problem

Parameter	Value
Length (m)	1.0
Number of meshes	100
Material	Sodium
Initial temperature (K)	370.94
Left boundary (K)	473.15
Right boundary	adiabatic

Figure 1 shows the calculation results when the melting front is at 0.3 m, where the temperature of heat source is 473.15 K (200 ℃).

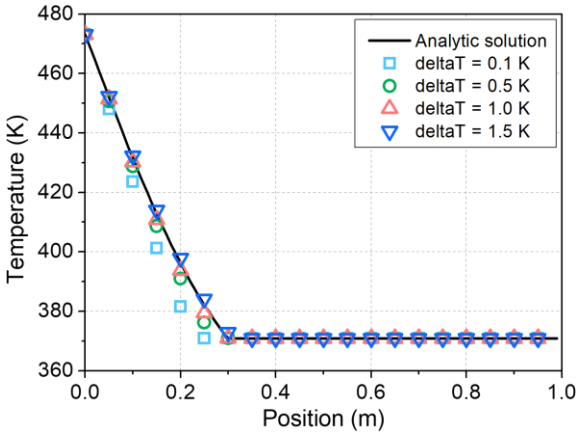

Figure 1. Calculation results of Stefan problem

From the calculation, deltaT = 1.0 K showed the best result, with maximum error of -3.07 K in temperature and less than 20 mm in melting front position, when melting front is at 0.3 m. Thus, the 2 K was chosen as the default value for the mushy zone temperature range.

3.2. Transient calculation with analytic solution

To verify the interfacial thermal resistances, transient analysis with analytic solution was conducted. Faghri & Harley [13] suggested 0-dimensional lumped parameter heat pipe transient calculation with an analytic solution, when input power is raised stepwise.

The analytic solution was compared to the average temperature of heat pipe considering the heat capacity of each cell in the 2-dimensional code. The calculation conditions are listed in Table 2.

Table 2. Conditions for transient calculation

Parameter	Value
Total length (m)	0.7
Evaporator length (m)	0.105
Adiabatic length (m)	0.0525
Condenser length (m)	0.5425
Vapor core diameter (cm)	1.4
Wick thickness (cm)	0.1
Wall thickness (cm)	0.1
Wick porosity	0.5
Working fluid	Sodium
Pipe material	Stainless steel
Initial temperature (K)	823.15

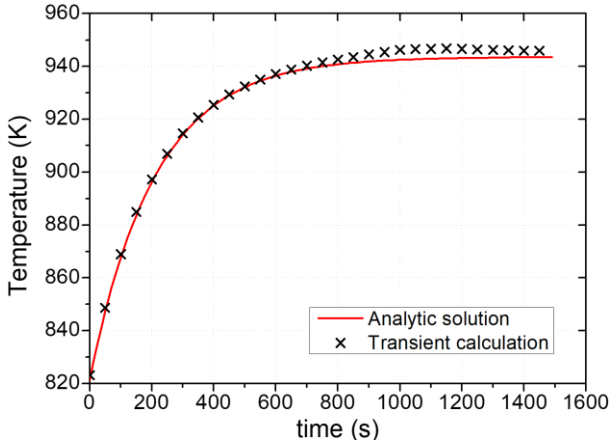

Figure 2. Transient calculation with an analytic solution

The transient calculation result is shown in Figure 2. It showed good agreement while in-house code showed slight overshooting and temperature drop at the end. This difference came from the delay in increase of heat removal at the condenser, compared to the temperature increase at the evaporator.

3.3. Validation of the improved code

To validate the code including both solid-liquid phase change model and interfacial thermal resistance, experimental data from heat pipe module for SAFE-30 reactor prototype was used [14]. The experiment was conducted by Los Alamos National Laboratory (LANL) with a sodium heat pipe to obtain temperature distribution during frozen start-up, transient operation, and shutdown. Calculation conditions are in Table 3.

Table 3. Conditions for transient calculation including start-up and shutdown

Parameter	Value
Heat pipe length (m)	1.20
Evaporator length (m)	0.43
Condenser length (m)	0.77
Heat pipe outer diameter (cm)	2.54
Heat pipe inner diameter (cm)	2.21
Wick type	Screen + Artery
Wick outer diameter (cm)	2.07
Wick inner diameter (cm)	1.74
Effective pore radius (μm)	47
Ambient Temperature (℃)	20.75

Figure 3 shows the calculation and experiment results, before and after implementing the start-up/shutdown model. Code with start-up/shutdown model showed higher accuracy compared to the previous code without the interfacial thermal resistance and solid-liquid phase change model. The results also showed when heat pipe vapor temperature is lower than 450 ℃, the temperature difference between evaporator and condenser becomes larger.

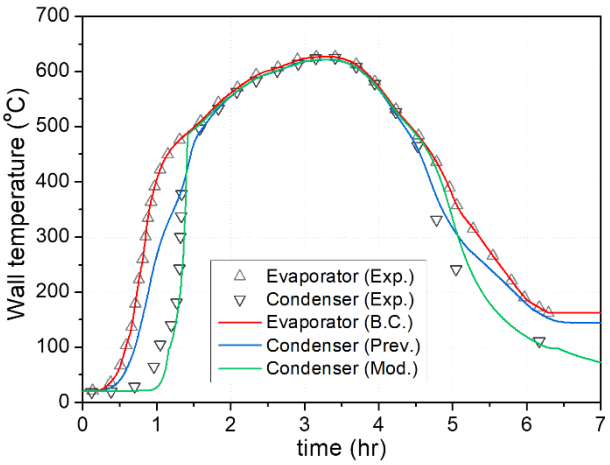

Figure 3. Transient analysis results

Figure 4 shows the heat pipe operation limits, and the heat transferred through the vapor core. During the start-up process, the heat pipe reached viscous limit, since the excessive heat was applied to the evaporator while the condenser did not reach the normal operation temperature. Viscous limit was exceeded during the shutdown period, after the temperature of condenser was cooled down. In both start-up and shutdown process, temperature difference between the evaporator and the

condenser became larger when the heat transfer was inhibited by the operation limits.

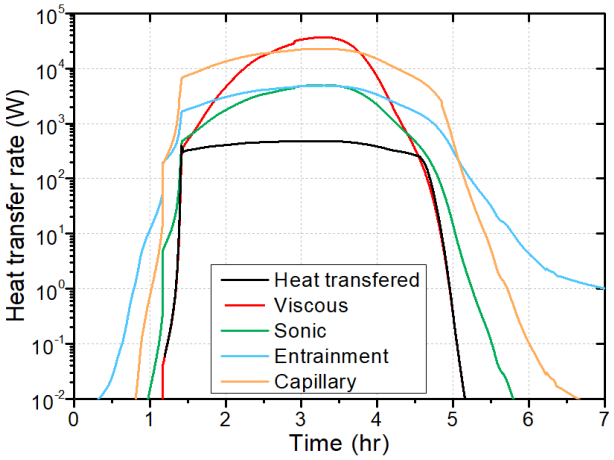

Figure 4. Heat transfer rate over time (improved code)

4. Conclusion

A start-up/shutdown model for 2-dimensional heat pipe code was developed and validated in this study. The start-up and shutdown behavior of heat pipe was considered by implementing solid-liquid phase change model and interfacial thermal resistance at wick-vapor interface. To verify each model, Stefan problem and lumped transient calculation are solved and they showed good agreement with the analytic solutions. Finally, transient analysis on heat pipe module test for SAFE-30 reactor was conducted for validation and showed improved simulation performance compared to the previous study, especially during start-up process.

However, iterative calculations for vapor core temperature showed slow convergence during start-up process since density and heat capacity of sodium vapor changed drastically at the low-temperature region. Therefore, future research will be conducted on solving mass and energy equations for vapor core for more accurate and stable calculation. Also, coupled calculations with other codes will be done to analyze multi-physics problems.

Acknowledgements

This work was supported by the National Research Foundation of Korea (NRF) grant funded by the Korean government (MSIT: Ministry of Science and ICT) (No. 2020M2D2A1A0206631723) and the National Research Council of Science & Technology (NST) grant by the Korea government (MSIT) (No. CAP23061-000).

REFERENCES

[1] V. Delmotte, Climate Change 2021: The Physical Science Basis. Contribution of Working Group I to the Sixth Assessment Report of the Intergovernmental Panel on Climate Change, Intergovernmental Panel on Climate Change (IPCC), Cambridge University Press, 2021.

[2] D. T. Wojtaszek, Potential Off-Grid Markets for SMRs in Canada, Canadian Nuclear Laboratories, Chalk River, Canada, 2017.

[3] D. R. Koenig, W. A. Ranken and E. W. Salmi, Heat-pipe reactors for space power applications, Journal of Energy 1, pp. 237-243, 1977.

[4] P. R. Mcclure, D. I. Poston, V. R. Dasari, and R. S. Reid, Design of Megawatt Power Level Heat Pipe Reactors, Los Alamos National Lab. (LANL, LA-UR-15-28840), Los Alamos, NM(United States), 2015.

[5] Y. Arafat, J. Van Wyk, eVinci Micro Reactor, Nuclear Plant Journal 37, pp.34-36, 2019.

[6] Y. H. Lee and H. K. Cho, Preliminary Development of Alkali Metal Heat Pipe Code for Microreactor Transient Analysis, 2022.

[7] J. S. Hsiao, An Efficient Algorithm for Finite-Difference Analyses of Heat Transfer with Melting and Solidification, Numerical Heat Transfer 8(6) pp. 653-666, 2007.

[8] P. Dunn and D. A. Reay, Heat Pipes, 2nd Edition, Pergamon Press, 1978.

[9] J. H. Jang, Startup characteristics of a potassium heat pipe from the frozen state. Journal of thermophysics and heat transfer, 9(1), pp.117-122, 1995.

[10] C. A. Busse, Theory of the Ultimate Heat Transfer Limit of Cylindrical Heat Pipes, Int. J. Heat Mass Transfer, Vol. 16, pp. 169-186, 1973.

[11] S. W. Chi, Heat pipe theory and practice: A sourcebook, Hemisphere Publishing, London, England, pp.79-95, 1976.

[12] M. N. Özışık, Heat conduction, John Wiley & Sons, NY(United States), pp. 392-408, 1993.

[13] A. Faghri, and C. Harley, Transient lumped heat pipe analyses. Heat Recovery Systems and CHP, 14(4), 351-363, 1994.

[14] R. S. Reid, J. T. Sena and A. L. Martinez, Sodium Heat Pipe Module Test for the SAFE-30 Reactor Prototype, AIP Conference Proceedings 552(1), American Institute of physics, pp.869-874, 2015.